ADAPTIVE BILATERAL FILTER FOR SHARPNESS ENHANCEMENT AND NOISE REMOVAL*

Buyue Zhang†

Texas Instruments Inc.
12500 TI Blvd., Dallas, TX 75243

Jan P. Allebach

School of ECE, Purdue University
West Lafayette, IN 47907

ABSTRACT

In this paper, we present an adaptive bilateral filter (ABF) for sharpness enhancement and noise removal. ABF sharpens an image by increasing the slope of the edges without producing overshoot or undershoot. Our new approach to slope restoration significantly differs from the previous slope restoration algorithms in that ABF does not involve detecting edge orientations or edge profiles. Compared with the bilateral filter, ABF restored images are significantly sharper. Compared with an unsharp mask (USM) based sharpening method – the Optimal USM (OUM), ABF restored edges are as sharp as those rendered by the OUM, but without halo. ABF also outperforms the bilateral filter and the OUM in noise removal.

Index Terms— bilateral filter, sharpness enhancement, noise removal, image restoration, slope restoration

1. INTRODUCTION

The problem we are interested in is twofold. First, we are very interested in developing a sharpening method that renders clean and crisp edges without halo. Second, we want to present a unified solution to both sharpness enhancement and noise removal.

In terms of noise removal, the conventional linear filter works well in smooth regions, but significantly blurs the edge structures of an image. A lot of research have been done on edge-preserving noise removal. One of the major endeavors in this area has been to utilize the rank order information [1, 2]. Due to a lack of the sense of spatial ordering, rank order filters generally do not suppress Gaussian noise optimally. In more recent years, a new approach to edge-preserving de-noising was proposed by Tomachi et al [3] and Smith et al [4]. Although their algorithms were developed independently, and named "SUSAN" filter and "bilateral filter" respectively, the essential idea is the same: enforcing both geometric closeness in the spatial domain and gray value similarity in the range in the de-noising operation. The edge-preserving de-noising bilateral filter proposed by Tomasi et al adopts a low pass Gaussian filter for both the domain filter and the range filter [3]. The domain low pass Gaussian filter gives higher weights to pixels that are spatially close to the center pixel. The range low pass Gaussian filter gives higher weights to pixels that are similar to the center pixel in gray value. Combining the range filter and the domain filter, a bilateral filter at an edge pixel becomes an elongated Gaussian filter that is oriented along the edge, which ensures that averaging is done mostly along the edge and is greatly reduced in the gradient direction. This is the reason why the bilateral filter can smooth the noise while preserving the edge structures.

In terms of image sharpening, USM remains the prevalent sharpening tool despite the drawbacks it has: First, USM sharpens an image by adding overshoot and undershoot to the edges which produces halo around the edges. Second, when applied to a noisy image, USM amplifies the noise in smooth regions which significantly impairs the image quality. To address the first problem, several slope restoration algorithms have been proposed [5, 6]. They either modify the edge profiles in the edge normal direction, or to simplify the problem, modify the 1D horizontal/vertical projection of the edge profiles. These 1D based slope restoration methods tend to produce artifacts in natural images and their effectiveness is not well demonstrated. The adaptive bilateral filter (ABF) we propose also aims to restore edge slope, but without the need to locate edge normals or obtain edge profiles. Therefore, ABF is efficient to implement. We will show in Sec. 4 that ABF produces clean, crisp, and artifact-free edges.

To address the second problem, locally adaptive sharpening algorithms have been proposed. Kim et al developed an Optimal Unsharp Mask (OUM) algorithm in which the strength of the USM is locally adaptive [7]. To obtain the optimal λ for different regions of the image, OUM classifies the pixels based on their response to a Laplacian of Gaussian (LoG) filter [7]. The optimal filter strength for each class is estimated by training with pairs of high quality original and the corresponding degraded images. Results show that OUM sharpens the detail areas as well as a conventional USM, while significantly reducing the noise in the smooth regions. Our proposed ABF algorithm is based on the bilateral filter. The parameters are optimized in a way similar to that of the OUM.

*Research supported by the Hewlett-Packard Company.

†This work was done while Buyue Zhang was a graduate student at Purdue University.

We will compare the results from ABF, OUM, and the conventional bilateral filter.

The rest of this paper is organized as follows: In Sec. 2, we present our ABF. In Sec. 3, the optimization of the parameters in ABF is described. In Sec. 4, the performance of ABF is evaluated and compared with that of the OUM and the bilateral filter. Finally, conclusions are given in Sec. 5.

2. THE ADAPTIVE BILATERAL FILTER (ABF)

The shift-variant filtering operation of the proposed ABF and its impulse response are shown in (1) and (2), respectively.

$$\hat{f}[m,n] = \sum_k \sum_l h[m,n;k,l] g[k,l]\,, \tag{1}$$

where $\hat{f}[m,n]$ is the restored image, $h[m,n;k,l]$ is the response at $[m,n]$ to an impulse at $[k,l]$, and $g[m,n]$ is the degraded image.

$$\begin{aligned} h[m,n;m_0,n_0] &= I(\Omega_{m_0,n_0}) r_{m_0,n_0}^{-1} e^{-\left(\frac{(m-m_0)^2+(n-n_0)^2}{2{\sigma_d}^2}\right)} \\ &\cdot \quad e^{-\frac{1}{2}\left(\frac{g[m,n]-g[m_0,n_0]-\zeta[m_0,n_0]}{\sigma_r[m_0,n_0]}\right)^2}, \end{aligned} \tag{2}$$

where $[m_0,n_0]$ is the center pixel of the window, $\Omega_{m_0,n_0} = \{[m,n] : [m,n] \in [m_0-N, m_0+N] \times [n_0-N, n_0+N]\}$, $I(\cdot)$ denotes the indicator function, and r_{m_0,n_0} normalizes the volume under the filter to unity.

Compared with the conventional bilateral filter given in [3], ABF contains two important modifications: First, an offset ζ is introduced in the range filter. Second, both ζ and the width of the range filter σ_r in ABF are locally adaptive. If $\zeta = 0$ and σ_r is fixed, ABF will degenerate into a conventional bilateral filter. For the domain filter, a fixed low pass Gaussian filter with $\sigma_d = 1.0$ is adopted in ABF. The combination of a locally adaptive ζ and σ_r transforms the bilateral filter into a much more powerful filter that is capable of both smoothing and sharpening. Moreover, it sharpens an image by increasing the slope of the edges. To understand how ABF works, we need to understand the role of ζ and σ_r in ABF.

The range filter can be interpreted as a one dimensional filter that processes the histogram of the image. We will illustrate this viewpoint for the window of data enclosed in the black box in Fig. 1 (a1), for which the histogram is shown in Fig. 1 (a2). For the conventional bilateral filter, the range filter is located on the histogram at the gray value of the current pixel and rolls off as the pixel values fall farther away from the center pixel value as shown in Fig. 1 (a2). By adding an offset ζ to the range filter, we are now able to shift the range filter on the histogram. As before, let Ω_{m_0,n_0} denote the set of pixels in the $(2N+1) \times (2N+1)$ window of pixels centered at $[m_0,n_0]$. Let MIN, MAX, and MEAN denote the operations of taking the minimum, maximum, and average value of the data in Ω_{m_0,n_0}, respectively. Let $\Delta_{m_0,n_0} = g[m_0,n_0] - \text{MEAN}(\Omega_{m_0,n_0})$. We will demonstrate the effect of bilateral filtering with a fixed domain Gaussian filter ($\sigma_d = 1.0$) and a range filter ($\sigma_r = 20$) shifted by the following choices for ζ.

1. No offset (conventional bilateral filter): $\zeta[m_0,n_0] = 0$,
2. Shifting towards the MEAN: $\zeta[m_0,n_0] = -\Delta_{m_0,n_0}$,
3. Shifting away from the MEAN, to the MIN/MAX:

$$\zeta[m_0,n_0] = \begin{cases} \text{MAX}(\Omega_{m_0,n_0}) - g[m_0,n_0], & \text{if } \Delta_{m_0,n_0} > 0, \\ \text{MIN}(\Omega_{m_0,n_0}) - g[m_0,n_0], & \text{if } \Delta_{m_0,n_0} < 0, \\ 0, & \text{if } \Delta_{m_0,n_0} = 0. \end{cases} \tag{3}$$

As we can see from Fig. 1, shifting the range filter towards MEAN(Ω_{m_0,n_0}) will blur the image (Fig. 1 (c1)). Shifting the range filter away from MEAN(Ω_{m_0,n_0}) will sharpen the image (Fig. 1 (d1)). In the case of operation No. 3, the range filter is shifted to the MAX or the MIN depending on Δ_{m_0,n_0}. The reason behind these observations is the transformation of the histogram of the input image by the range filter. In our case, the data window Ω_{m_0,n_0} marked in Fig. 1 (a1) contains an edge. Therefore, the histogram of the data window contains two peaks, as shown in (a2), which correspond to the darker and brighter sides of the edge, respectively. Any pixels located between the two peaks appear on the slope of the edge. The conventional bilateral filter without offset does not significantly alter the histogram or edge slope, as shown in (b2) and (b3), respectively. Shifting the range filter to MEAN(Ω_{m_0,n_0}) at each pixel will redistribute the pixels towards the center of the histogram, as shown in (c2). Hence the slope is reduced, as shown in (c3). On the other hand, if we shift the range filter further away from the MEAN(Ω_{m_0,n_0}), pixels will be compressed against the two peaks, as shown in (d2). The slope will be increased, as shown in (d3). We need to point out here that shifting the range filter based on Δ_{m_0,n_0} is very sensitive to noise. In Sec. 3, we will describe a different strategy for choosing ζ that is much more reliable.

The parameter σ_r of the range filter controls the width of the range filter. If σ_r is large compared to the range of the data in the window, the range filter will assign similar weights to every pixel in the range. Therefore, it does not have much effect on the overall bilateral filter. On the other hand, a small σ_r will make the range filter dominate the bilateral filter. By making ζ and σ_r adaptive and jointly optimizing both parameters, we transform the bilateral filter into a much more powerful and versatile filter. To smooth a pixel, we can shift the range filter towards MEAN(Ω_{m_0,n_0}), and/or use a large σ_r which enables the spatial Gaussian filter to take charge in bilateral filtering. To sharpen a pixel, we can shift the range filter away from MEAN(Ω_{m_0,n_0}) towards MAX(Ω_{m_0,n_0}) or MIN(Ω_{m_0,n_0}), depending on whether it is above or below the midpoint of the edge slope. At the same time, we reduce σ_r accordingly. With a small σ_r, the range filter dominates the bilateral filter and effectively pulls up or pushes down the pixels on the edge slope.

3. OPTIMIZATION OF ABF PARAMETERS

The parameter optimization is formulated as a Minimum Mean Squared Error (MMSE) estimation problem. We classify the pixels into T classes, and estimate the optimal ζ and σ_r for each class that minimizes the overall MSE. Let P be the total number of training image sets. The $k-th$ set ($k = 1, 2, ..., P$) consists of an original image $f_k[m,n]$, a degraded image $g_k[m,n]$, the class index image $L_k[m,n]$, and the restored image $f_k[m,n]$. All four of these images have dimensions $M_k \times N_k$. Let

$$\mathcal{S}^{(k)} = \{[m,n] \,:\, [m,n] \in [0, M_k - 1] \times [0, N_k - 1]\}\,, \quad (4)$$

be the set of indices for the pixels in these images. Also let

$$\mathcal{S}_i^{(k)} = \{[m,n] \,:\, L_k[m,n] = i \text{ and } [m,n] \in \mathcal{S}^{(k)}\}\,, \quad i = 1, 2, ..., T, \quad (5)$$

Given the P training image sets as described above, the optimal parameters $\{\vec{\zeta}^*, \vec{\sigma_r}^*\}$ satisfy:

$$\{\vec{\zeta}^*, \vec{\sigma_r}^*\} = \arg\min_{\{\vec{\zeta}, \vec{\sigma_r}\}} \sum_{k=1}^{P} \|f_k[m,n] - \hat{f}_k[m,n]\|^2_{\mathcal{S}^{(k)}}\,, \quad (6)$$

where $\|A\|_B^2$ denotes the L-2 norm of the array A over the index set B, $\vec{\zeta} = \{\zeta_i : i = 1, 2, ..., T\}$, and $\vec{\sigma_r} = \{\sigma_{r,i} : i = 1, 2, ..., T\}$.

Since the classes are independent and non-overlapping, we can estimate the optimal $\vec{\zeta}$ and $\vec{\sigma_r}$ for each class individually by replacing $\mathcal{S}^{(k)}$ in the norm on the right side of (6) by $\mathcal{S}_i^{(k)}$, and $\{\zeta^*, {\sigma_r}^*\}$ on the left side by $\{{\zeta_i}^*, {\sigma_{r,i}}^*\}$, $i = 1, 2, ..., T$.

We used five training images to estimate ζ and σ_r. The high quality original images are from the training images used in OUM. The degraded images are generated by a blur point spread function (PSF) and a tone-dependent noise model. Both the training images and the degradation process are described in [7]. Each pixel in the degraded image is classified by a 9×9 LoG operator with $\sigma = 1.5$ [7]. The LoG class number $L_k[m,n]$ at pixel $[m,n]$ is the LoG response rounded to the nearest integer. For pixels with LoG response greater than 60 or less than -60, the class number is set to be 60 and -60, respectively. Figure 2 shows the resulting optimal parameters.

4. RESULTS AND DISCUSSIONS

The performance of ABF is evaluated with the image "Kids". Kids was taken by a Canon Autoboy-A automatic analog camera, printed as a 4×6 in^2 photo, and scanned at 600 dpi [7]. In Fig. 3, we zoom in to compare the rendering of the smooth regions, the edges, and the textured areas. Figure 3 (b) shows ABF is the most effective one in removing the noise on the girl's shirt. The conventional bilateral filter reduces noise, but does not restore the sharpness of the image. Both ABF and OUM significantly sharpen the edges of the text. However, the text on the boy's shirt rendered by ABF does not have the halo that appears in the OUM restored image. Both ABF and OUM are able to sharpen the grass in the background. The OUM rendered grass looks more contrasty; but the contrast of ABF rendered grass is closer to that of the original image. Figure 3 (c) shows the edge profiles at edge pixel A inside the right marked region in Fig. 3 (a). The bilateral filter does not change the slope of the edge. The OUM increases the slope but results in large overshoot and undershoot. The ABF enhances the slope the most without generating overshoot and undershoot around the edges.

5. CONCLUSIONS

In this paper, we present an adaptive bilateral filter (ABF) which is developed in the framework of the conventional bilateral filter. ABF outperforms the bilateral filter in noise removal. At the same time, it renders significantly sharper images. Compared with an USM based adaptive sharpening method – OUM, ABF stored edges are as sharp as the OUM restored edges, but without the halo artifacts that OUM produces. Our new approach to slope restoration does not involve edge orientation estimation or edge profile extraction. It is therefore efficient to implement.

6. REFERENCES

[1] J. W. Tukey, "Nonlinear (nonsuperposable) methods for smoothing data," in *1974 EASCON Conf. Rec.*, 1974, p. 673.

[2] A Bovik, T. Huang, and D. Munson, "Image restoration using order-constrained least-squares methods," in *Proc. ICASSP '83*, 1983, pp. 828– 831.

[3] C. Tomasi and R. Manduchi, "Bilateral filtering for gray and color images," in *Proc. 6th IEEE Int Conf Comput Vision*, 1998, pp. 839 – 846.

[4] S. M. Smith and J. M. Brady, "SUSAN - a new approach to low level image processing," *Int J Comput Vision*, vol. 23, no. 1, pp. 45 – 78, 1997.

[5] A. Das and R. M. Rangayyan, "Enhancement of image edge sharpness and acutance," in *Proc. SPIE*, 1997, vol. 3026, pp. 133 – 142.

[6] J. Tegenbosch, P. Hofman, and M. Bosma, "Improving nonlinear up-scaling by adapting to the local edge orientation," in *Proc. SPIE*, 2004, vol. 5308, pp. 1181 – 1190.

[7] S. Kim and J. P. Allebach, "Optimal unsharp mask for image sharpening and noise removal," *J Electron Imaging*, vol. 14, no. 2, pp. 023007–1 – 023007–13, 2005.

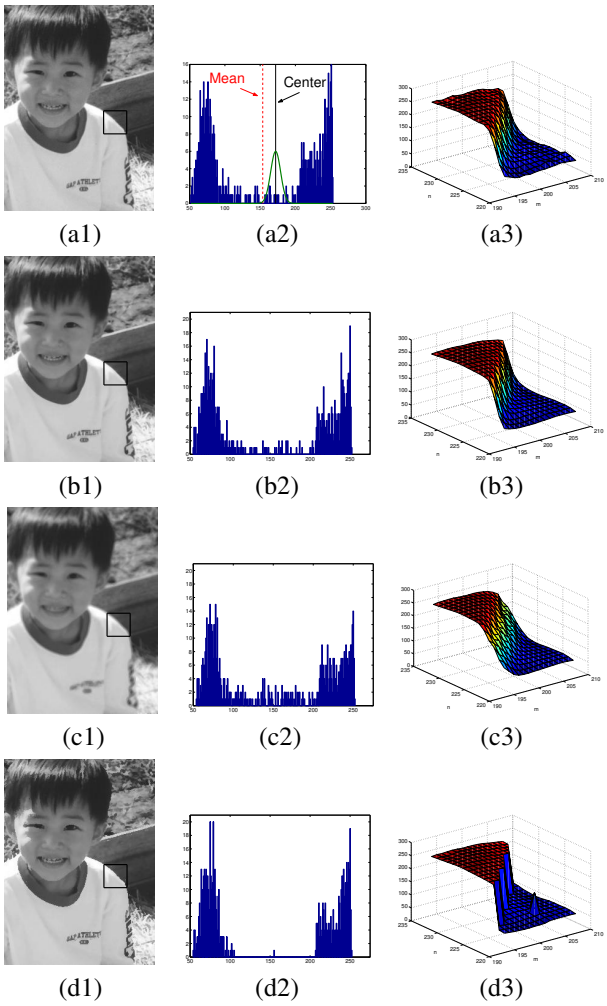

Fig. 1. Illustration of the effect of bilateral filtering with a fixed domain Gaussian filter ($\sigma_d = 1.0$) and a range filter ($\sigma_r = 20$) with the three choices of ζ described by operations No. 1 (2nd row), No. 2 (3rd row), and No. 3 (4th row). (a1) The degraded image "Boy", the black box marked on the "Boy" denotes a 25×25 data window Ω_{m_0,n_0}. (a2) The histogram of the image data in Ω_{m_0,n_0}. The range filter at the center pixel $[m_0, n_0]$, MEAN(Ω_{m_0,n_0}), and $g[m_0, n_0]$ are marked on the histogram; (a3) The 3D plot of the data in Ω_{m_0,n_0}. Starting with the second row, the first column illustrates the restored images from the three operations; the second column shows the resultant histograms of Ω_{m_0,n_0}; and the last column shows the 3D plots of the filtered data in Ω_{m_0,n_0}.

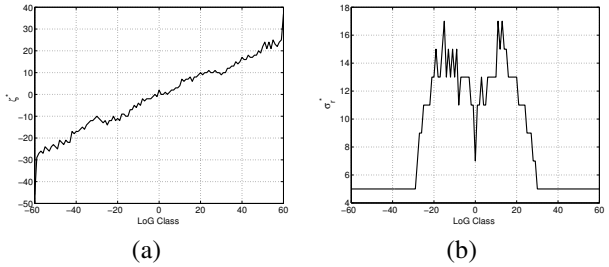

Fig. 2. The estimated optimal parameters for each class. (a) Optimal ζ, (b) optimal σ_r.

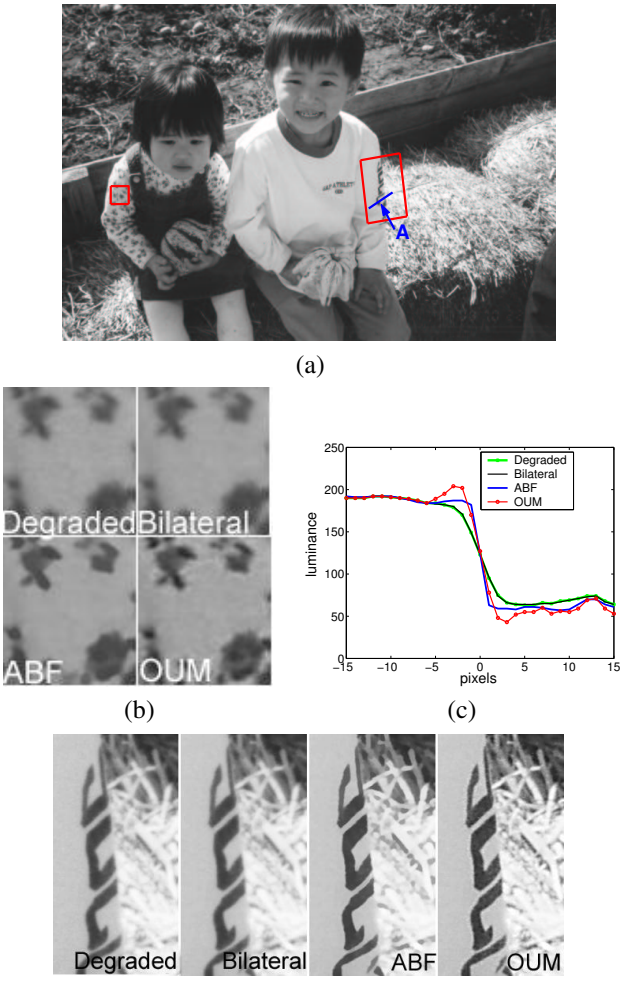

Fig. 3. Results: (a) Test image "Kids": 3439×2344. The regions inside the two boxes in (a) will be zoomed in to compare results from bilateral filter ($\sigma_r = 5$ and $\sigma_d = 1$), OUM, and ABF; (b) zoom in of the left marked region in (a); (c) edge profiles taken at an edge pixel "A" inside the right marked region in the degraded image, the bilateral restored image, the ABF restored image, and the OUM restored image; (d) zoom in of the right marked region in (a).